I.A.U
Karaj branch

Journal of
A p p l ied
C hemical
R esearch
jacr.kiau.ac.ir

Journal of Applied Chemical Research, 17, 2, 61-81 (2023)

Application of CM-β-CD-Fe_3O_4NPs: As an Adsorbent for the Removal of Aluminum ion from Wastewater

Amir Abbas Ghazali, Farzaneh Marahel*, Bijan Mombeni Goodajdar

Department of Chemistry, Omidiyeh Branch, Islamic Azad University, Omidiyeh, Iran

(Received 05 Aug. 2022; Final revision received 19 Nov. 2022)

Abstract

The applicability of CM-β-CD-Fe_3O_4NPs synthesis for the removal of Aluminum ion from wastewater was studied. The active sites and morphology structure of CM-β-CD-Fe_3O_4NPs synthesis were analyzed using BET, FT-IR, XRD, SEM, and XPS respectively. The effect of independent variables namely pH, adsorbent dosage, contact time, Al (III) ion concentration in solution, were investigated through batch experiments, and to be 7, 50 mg L^{-1}, 0.1 g and 90 min for the adsorption of Al (III) ion onto CM-β-CD-Fe_3O_4NPs sorbent were found respectively. The adsorbed Al (III) ion onto the CM-β-CD-Fe_3O_4NPs showed excellent fitting to the pseudo-first-order adsorption kinetic with a correlation coefficient value of 0.999. Meanwhile, the experimental equilibrium data were fitted to the conventional isotherm models accordingly. Freundlich isotherm has good applicability for the experimental data with a maximum adsorption capacity (q_{max}) of 35.88 mgg^{-1} for Al (III) ion onto CM-β-CD-Fe_3O_4NPs. The overall results confirmed that CM-β-CD-Fe_3O_4NPs could be a promising adsorbent material for Al (III) ion removal from wastewater treatment.

Keywords: Aluminum ion, Adsorption Capacity, CM-β-CD-Fe_3O_4NPs, Kinetic, Wastewater.

Corresponding author: Farzaneh Marahel, Department of Chemistry, Omidiyeh Branch, Islamic Azad University, Omidiyeh, Iran. Email: Farzane.marahel.fm@gmail.com.*

Introduction

Wastewater contaminated from discharges of industrial and domestic in general embodies different types of heavy metals like aluminum, cobalt, nickel, cadmium, lead, and zinc. The absorption of heavy metals by living organisms is due to their excessive solubility in aquatic mediums. Ingestion of large amounts of heavy metals and their accumulation in body can cause serious health disorders if they enter the food chain [1,2]. Heavy metal removal from effluent can be achieved by conventional treatment processes such as chemical precipitation, ion exchange, and electrochemical removal. These processes have significant disadvantages, including complex equipment, high energy consumption, and the generation of toxic sludge [2,3].

Aluminum (Al) is widespread throughout nature, air, water, plants, and consequently in all the food chain [4]. Nevertheless, the excessive ingestion of aluminum can influence negatively the human organism disturbing calcium and phosphate metabolisms and thus damaging the bone system. Moreover, the accumulation of high amounts of aluminum in the brain is associated with Alzheimer's disease, senescence symptoms, and amnesia in young people [5]. For that reason, removal of Aluminum (Al) ions in drink waters is crucial for guaranteeing consumers' health [6,7]. Diverse quantitative analytical method has been reported among in determining Aluminum (Al) ions in waste water including: Spectrophotometric [8], solid-phase extraction [9], kinetic-spectrophotometry [10], and Flow injection [11], cloud point extraction (CPE) [12], and fluorescent [13]. Therefore, finding an easy, economical and effective method for wastewater treatment has emerged as a hot topic in scientific community [14,15].

Adsorption is a diverse process and is extensively used to remove contaminants from wastewater. Its popularity is due to advantages including higher efficiency lower waste, and facile and mild operational conditions. The successfulness of adsorption techniques in the deletion of pollutants especially those which are extremely stable in the biological degradation process via economically accomplishable mild ways [15-18].

The most significant benefits of adsorption are that the residual contaminants are eliminated during the adsorption phase [19,20]. With the addition of metal oxide nanoparticles to the polymer matrix many benefits exist for adsorption and removal of pollutants. Iron nanoparticles include a large surface area, being widely accessible, being stable in an acidic/basic environment, and having a stable structure at high temperatures one of the most widely used nanoparticles is the adsorption process [21-23]. *Cyclodextrins* (CD) can be produced from starch using enzymes like amylase, malting and mashing. The α-, β- and γ-

cyclodextrins contain respectively 6, 7 and 8 glucopyranose units, with primary and secondary hydroxyl groups located in the structure. Dextrin has attracted the attention of researchers because of its chemical structure, water-solubility, biodegradability, biocompatibility, affordability, abundance, and ability to produce applied materials [24,25]. Therefore, preparing *cyclodextrin*/Fe_3O_4NPs, especially as an effective adsorbent and alternative to exorbitant or noxious adsorbents for the elimination of Al (III) ion from wastewater treatment attracted our attention [26-28].

After synthesizing CM-β-CD-Fe_3O_4NPs as a unique adsorbent, its characterization by Fourier transform infrared spectroscopy (FTIR), scanning electron microscopy (SEM), and X-ray diffraction (XRD) analysis has been carried out. The effects of important variables like pH, adsorbent dosage, contact time, and Al (III) ion concentration optimized. Varied isotherm models, namely Freundlich, Langmuir, Temkin, and Brunoire, Emmett, and Teller were applied to fit the experimental equilibrium data. Considering the kinetic models of pseudo-first-order, the pseudo-second-order models confirmed the dominance of the pseudo- first-order model in the kinetic of adsorption process. The capability of CM-β-CD-Fe_3O_4NPs in eliminating of Al (III) ion from wastewater treatment was demonstrated by evidences.

Experimental

Materials and Instrumentation

All the chemicals used are of the highest purity, and purchased from Merck (Darmstadt, Germany). Aluminum hydroxide (99%), *Cyclodextrin* (99%), and Iron oxide (98.0%). The standard and experimental solutions were obtained by diluting the stock solutions with deionized water. Atomic Absorption Spectrophotometer Shimadzu 6800 with air-acetylene flame equipment (Shimadzu Company, Japan). Fourier transform infrared (FT-IR) spectra was from PerkinElmer (FT-IR spectrometer BX, Germany). Scanning electron microscopy (SEM, Phillips, PW3710, Netherland), used to study the morphology of samples.

Preparation CM-β-CD-Fe_3O_4NPs

Fe_3O_4NPs were prepared by mixing $FeCl_2{\cdot}4H_2O$ (2.74 g), $FeCl_3{\cdot}6H_2O$ (3.11 g) and 0.85 mL concentrated hydrochloric acid into 25 mL deionized water, and 40 ml of NH_4OH (25%) was to 1.5 g CM-β-CD in 40 ml to was added slowly. The added to a NaOH solution (1.5 M). In the during the whole process, for the synthesis of CM-β-CD-Fe_3O_4NPs, the solution temperature was maintained at 80ºC, and introducing nitrogen gas through a sparer into the

solution for oxygen removal [26]. After completion of the reaction, the obtained Fe_3O_4NPs were separated from the reaction medium by the magnetic field, then we increased the bath temperature to 90°C. The sediment suspension was stirred for 3 hours. Stirring was stopped and the suspension was placed in the laboratory for 2 hours. The CM-β-CD-Fe_3O_4NPs with an equal weight ratio and after analysis, BET, XRD, FT-IR and SEM were used as adsorbent.

A typical adsorption experiment

Generally, the batch method is currently used in adsorption studies. 250 mL solution having (50 mg L^{-1}), the concentration of Al (III) ion was prepared and the effect of parameters affecting the removal Al (III) ion including the initial concentration of the ion, pH, dosage sorbent in the range (0.01 to 1.0 g), time intervals (30, 40, 60, 80, 90, 100, 120 min) was agitated at a constant rate of 200 rpm in a temperature-controlled orbital shaker maintained at 30±1^{o}C was studied in the process. The analysis of the dilute phase was done for determining Al (III) ion concentration using a Shimadzu 6800 Atomic absorption spectrophotometer, and the equilibrium concentrations and removal efficiency (%) of the Al (III) ion were calculated according to equations (1) and (2), respectively. Meanwhile, all experiments were performed five times, and final results were presented as mean values.

$$R\% = \frac{C_0 - C_e}{C_0} \times 100 \qquad (1)$$

$$q_i = \frac{V(C_0 - C_e)}{M} \times 100 \qquad (2)$$

C_0 (mg L^{-1}) in the formula refers to the initial Al (III) ion concentration and C_e (mg L^{-1}) represents the equilibrium Al (III) ion concentration in aqueous solution. V (L) shows the solution volume and W (g) signifies the mass adsorbent [21,30].

Results and discussion

BET analysis of CM-β-CD-Fe_3O_4NPs

As Figure 1 demonstrates, the pore structure parameters of molecular sieve materials such as N_2 adsorption-desorption isothermal curve and specific surface area were determined by micromeritics ASAP2010M adsorption analyzer. The sample was dropped onto the slide for conducting layer treatment, at 77 K liquid nitrogen temperature and the operating voltage was 20 KV. The specific surface area was calculated using the BET (Brunner-Emmett-Teller) method, while the pore size distribution was calculated using the BJH (Barrett–Joyner–Helena) equation [29].

The relevant data involved in the calculation of each parameter were obtained according to the adsorption branch of nitrogen adsorption-desorption isotherms of each sample prepared experimentally. The adsorption capacity of CM-β-CD-Fe_3O_4NPs depends on porosity and chemical reactivity of functional groups at the surface. Knowledge of surface functional groups would give insight into the adsorption capability of the CM-β-CD-Fe_3O_4NPs.

Table 1. BET surface area and pore volume of the CM-β-CD and CM-β-CD-Fe_3O_4NPs.

Property	Samples	
	CM-β-CD	**CM-β-CD-Fe_3O_4NPs**
BET surface area (m^2/g)	31.02	60.95
Langmuir surface area (m^2/g)	31.93	63.56
t-Plot micropore area (m^2/g)	27.39	55.18
V_{total} ($cm^3\ g^{-1}$)	0.09492	0.1624
Mean pore diameter (nm)	12.28	10.66

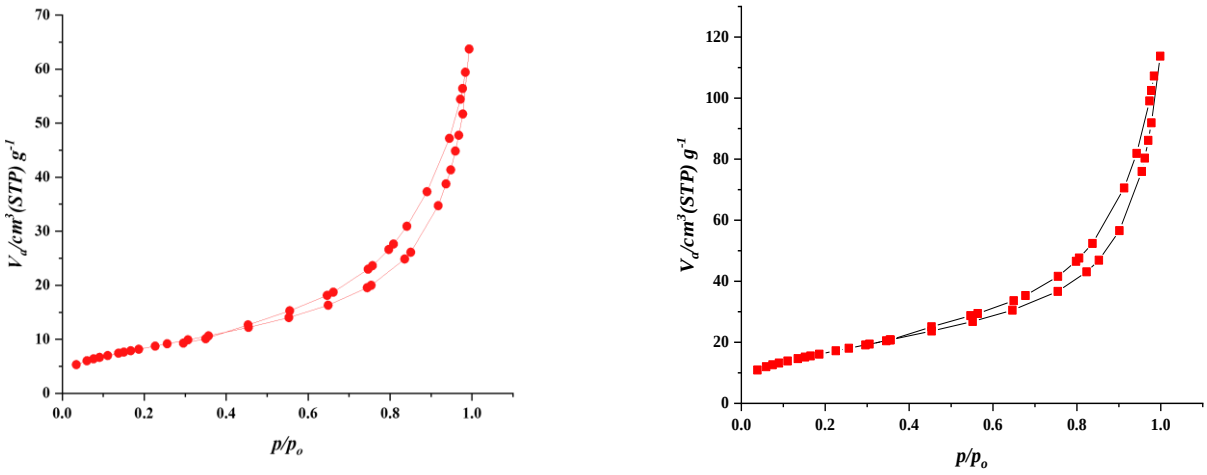

Figure 1. N_2 gas adsorption/desorption isotherms of CM-β-CD and CM-β-CD-Fe_3O_4NPs.

Sample characterization of adsorbent

The FTIR spectra of CM-β-CD and CM-β-CD-Fe_3O_4NPs in the 500–4000 cm^{-1} wave number range, as demonstrated in Figure 2a, the FTIR spectrum of CM-β-CD-Fe_3O_4NPs presents clear peak at 876.3 and 580.0 cm^{-1} related to Fe–O. The 2921.68 cm^{-1} band can be regarded as being caused by C–H stretching in CM-β-CD system, the peaks at 1120.23 and 1123.8 cm^{-1} corresponded to C–O–C and C–C bonds, the incorporation of the carboxyl methyl group (–$COOCH_3$) into CM-β-CD molecule (Figure 2a).

The novel emerging signal at 3567 cm^{-1} can be attributed to –OH stretching [32]. XRD patterns of the sample are shown in (Fig. 2b), confirm the spherical structure of CM-β-CD-

Fe_3O_4NPs. As can be seen, the entirely crystalline structure is confirmed, while the high intensity of peak at 38.8° (311) indicates the presence of a low quantities of substances in an amorphous condition [33]. The morphological properties of CM-β-CD-Fe_3O_4NPs was investigated by FE-SEM and is exhibited in Figures 2c and 2d, the evenness, homogeneity, orderliness and approximate uniformity of synthesized CM-β-CD-Fe_3O_4NPs, can be observed. CM-β-CD-Fe_3O_4NPs after surface modification came to be uneven, bigger and agglomerate**.** It can be seen that the particles are mostly spherical with the various size distribution as they form agglomerates. Based on the particle size distribution, we obtained the average particle size in the range of 12-25 nm very close to those determined by XRD analysis [34].

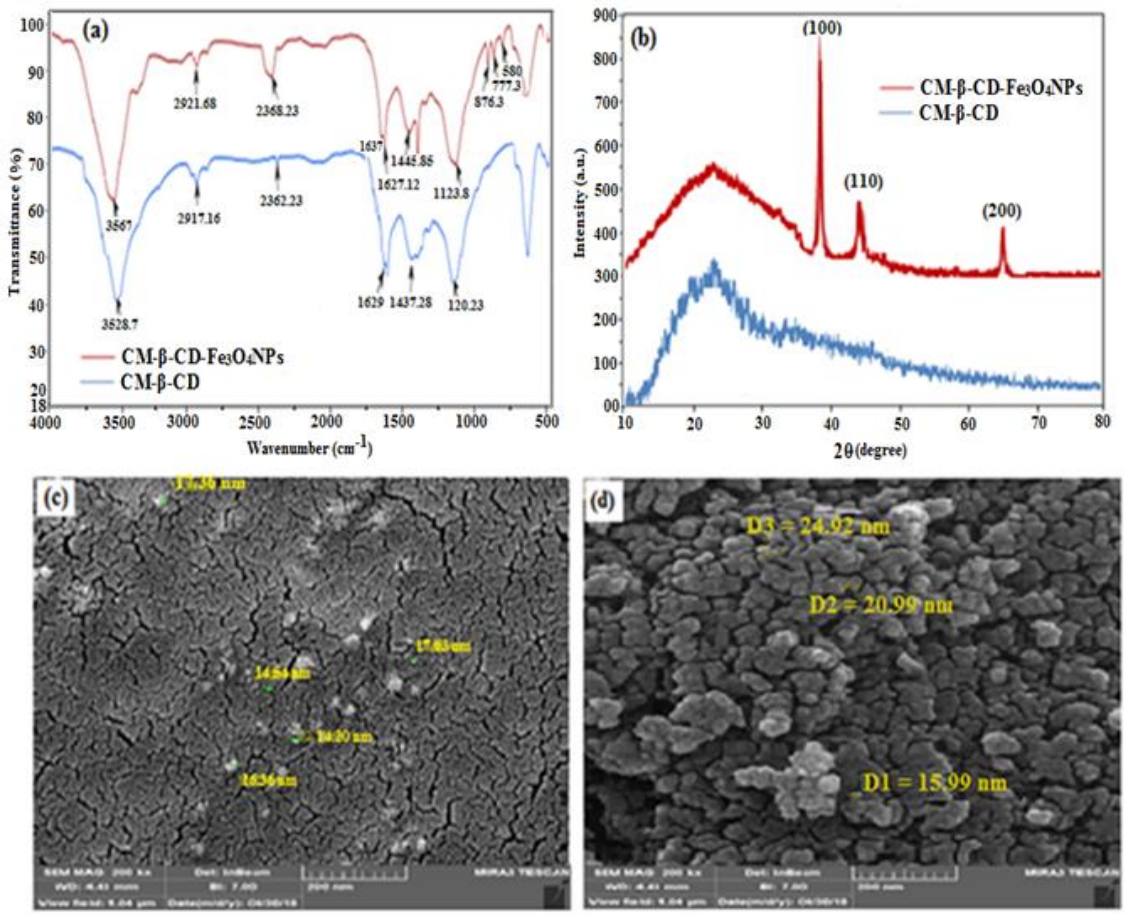

Figure 2. (a) FT-IR spectrum (b) XRD pattern (c and d) SEM image of the prepared of CM-β-CD and CM-β-CD-Fe_3O_4NPs.

XPS analysis

XPS analysis was applied to find the chemical binding in the as-synthesized CM-β-CD-Fe_3O_4NPs. The C 1s de convoluted spectrum is shown in Figure 3. The C 1s spectrum can be curve-fitted into four peak components with a binding energy of about 284.6, 286.1, 287.9 and 288.7 eV, attributable to the carbon atoms forms of C=C (aromatic), C-O (alcoholic hydroxyl and ether), C=O (carbonyl) and COO-(carboxyl and ester) species, respectively. The C-O/C-O-C and C=O peaks are the characteristic peaks of CM-β-CD polymer. Moreover, the presence of a COO- peak at 288.7 eV indicates that the COOH functional groups on the CM-α-CD polymer reacted with surface OH groups to form metal carboxylate (COOM) [26].

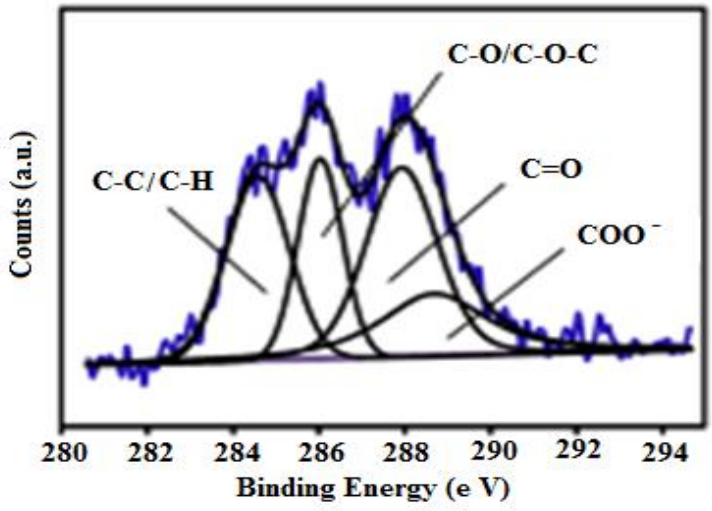

Figure 3. XPS pattern of polymer CM-β-CD-M.

Effect of pH on the adsorption

Deletion of Al (III) ion onto sorption CM-β-CD-Fe_3O_4NPs as a function of pH by varied sorbent is shown in (Figure 4). The highest deletion percentages of Al (III) ion was procured at pH 7.0. Abatement in Al (III) ion deletion at pH <7 happened due to competition of Al (III) ion with H^+. Additionally, in highly acidic pH, sharp concentration of H^+ set the scene for protonation of nitrogen atoms on the surface of adsorbents and provoked the reduction of interaction with Al (III) ion and the surface of adsorbents. Both reasons of the precipitation of hydroxide and conversion of Al (III) ion provoked the reduction in Al (III) ion deletion at pH >7. This phenomenon obstructed the access of Al (III) ion to adsorption sites and culminated in less adsorption of Al (III) ion onto sorption CM-β-CD-Fe_3O_4NPs [35,36].

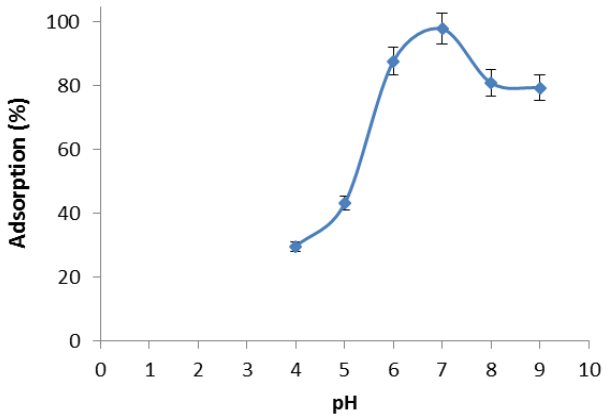

Figure 4. Effect of pH on the adsorption of Al (III) ion [Al (III) ion = 50.0 mg L^{-1}; dosage sorbent = 0.1 g; time = 90.0 min].

Effect of the dosage of absorbent

Adsorption of Al (III) ion was studied using different dosages of CM-β-CD-Fe_3O_4NPs (0.01-1.0 g) at the optimum. At low adsorbent dosages, the absorbent surface became saturated with the metal ions and the residual metal ion concentration in the solution was large. As the adsorbent dosage increases, the adsorbent sites available for Al (III) ion are also increased and consequently better adsorption takes place. However, higher dosages (>0.1 g) had no significant effect on the metal ions uptake as the surface Al (III) ion concentration and the solution metal ions concentration came to equilibrium with each other. The maximum removal of metal ions was obtained for the adsorbent dosage of 0.1 g, as shown in (Figure 5). Accordingly, a 0.1 g dosage of CM-β-CD-Fe_3O_4NPs was used in all subsequent experiments [37,38].

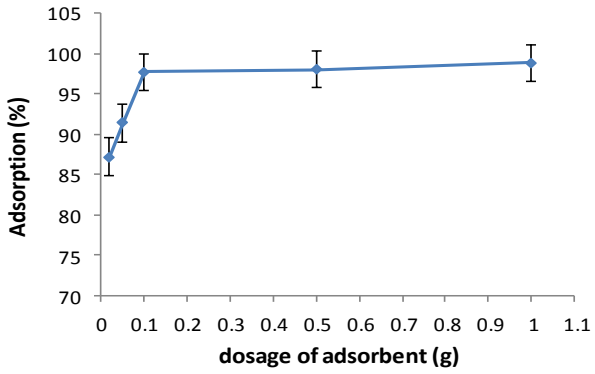

Figure. 5: Effect of the dosage of absorbent on the adsorption of Al (III) ion [Al (III) ion = 50.0 mg L^{-1}; pH =7.0; time = 90.0 min].

Effect of the contact time on the adsorption

The impact of contact time on the sorption of Al (III) ion with sorbent was examined. The removal of Al (III) ion was scrutinized in batch experiments applying 30 to 120 min contact

time, pH value 7 for Al (III) ion 50.0 mg L^{-1}, 0.1 g adsorbent dosage. Figure 6, show the effect of contact time on the removal of Al (III) ion onto CM-β-CD-Fe_3O_4NPs [39].

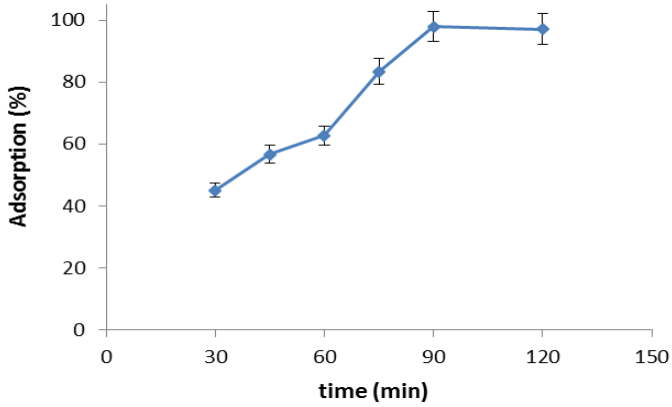

Figure 6. Effect of contact time o on the adsorption of Al (III) ion [Al (III) ion = 50.0 mg L^{-1}; pH =7.0; dosage sorbent = 0.1 g].

Effect of temperature on adsorption

Temperature is anticipated to have an influence on the ion adsorption properties of CM-β-CD-Fe_3O_4NPs adsorbent with Al (III) ion. The effect of temperature on the ions adsorption properties at 305.15 to 338.15 K with a fixed initial Al (III) ion concentration of 50 mg L^{-1} was investigated, as shown in (Figure 7). The adsorption capacity of the sorbent increased when the temperature increased from 305.15 to 338.15 K. The uptake of Al (III) ion onto CM-β-CD-Fe_3O_4NPs was rapid initially and then slows down gradually until equilibrium was attained, after that there was not significantly increased in the Al (III) ion uptake. This can be partly attributed to strong attractive forces between Al (III) ions at higher temperatures [39], along with the contributions due to the solution of the sorbent surface. It can also be said that the reaction of Al (III) ion and surface functional groups is enhanced by the increased temperature of the reaction [40].

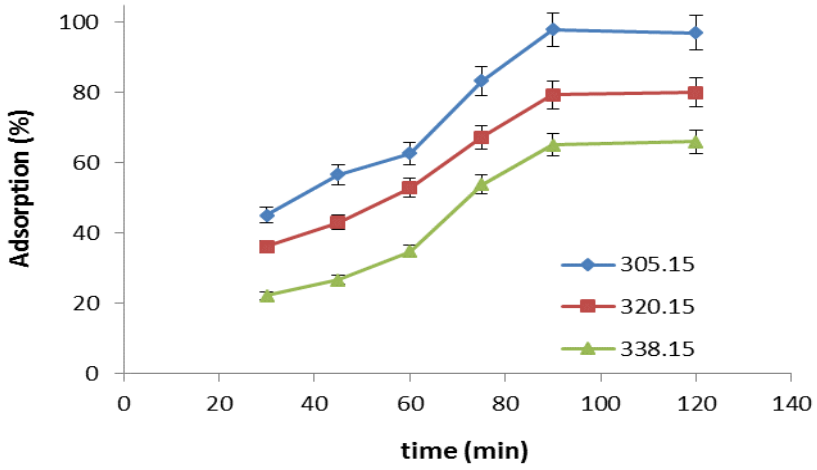

Figure 7. Effect of temperature on the adsorption of Al (III) ion [Al (III) ion = 50.0 mg L^{-1}; pH =7.0; dosage sorbent = 0.1 g].

A comparative study

The adsorption percent of Al (III) ion onto each of Fe_3O_4NPs, CM-β-CD, and CM-β-CD-Fe_3O_4NPs was evaluated at the optimum condition and the obtained results are represented in (Figure 8). As was can see, the trend of the effectiveness of mentioned adsorbents for removing Al (III) ion from aqueous media as follow: CM-β-CD-Fe_3O_4NPs (96.0%)> CM-β-CD (70.0%)> Fe_3O_4 NPs (64.4%).

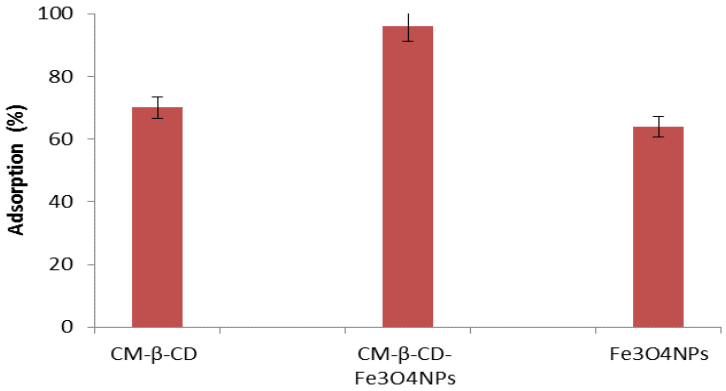

Figure 8. Comparison of the effectively of Fe_3O_4NPs, CM-β-CD and CM-β-CD-Fe_3O_4NPs [Al (III) ion conc = 50.0 mg L^{-1}; pH = 7; adsorbent dosage = 0.1g; time = 90.0 min; stirring speed = 200 rpm].

Error analysis

The chi square (X^2) tests were adopted to determine the suitability of the isotherm model with respect to the experimental data. The X^2 equation is as follows:

$$\chi 2 = \sum \frac{(q_e - q_{e,m})^2}{q_{e,m}} \qquad (3)$$

Where q_e (mgg^1) is the experimental equilibrium capacity and q_e, m (mgg^1) is the equilibrium capacity obtained from the model [36,41].

Adsorption isotherms

The adsorbate molecules division among the solid and liquid phases in equilibrium is designated based on the isotherms of adsorption. Adsorption of Al (III) ion onto CM-β-CD-Fe_3O_4NPs was modeled based on four adsorption isotherms of Freundlich, Langmuir, Temkin and Brunoire, Emmett, and Teller isotherms [42].

1) The Langmuir isotherm assumes monolayer adsorption on a homogeneous surface with a restricted number of adsorption sites [42]. Therefore, when a site is occupied, no further sorption can occur at that site. Consequently, the saturation point is equal to the maximum adsorption of the surface. The linearized form of the Langmuir isotherm model is as follows:

$$\frac{C_e}{q_e} = \frac{1}{K_L q_{\max}} + \frac{1}{q_{\max}} C_e \qquad (3)$$

In relation (3) q_m: is the value of monolayer adsorption capacity in Langmuir model and K_L: constant value of Langmuir (mg L^{-1}). Increasing the amount of adsorbent caused a considerable increase in the adsorbed ions amounts (Figure 9).

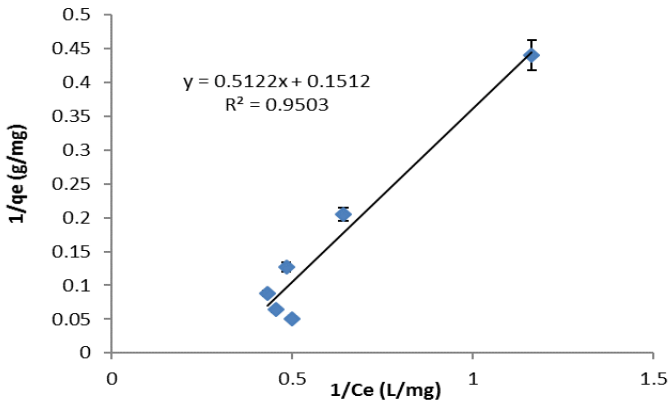

Figure 9. Langmuir isotherm for the adsorption percent Al (III) ion [Al (III) ion = 50 mg L^{-1}; pH =7.0; dosage sorbent = 0.1 g; time = 90.0 min].

Freundlich isotherm model is the more for the adsorption of components dissolved in a liquid solution, it is assumed that: First, the adsorption is monolayer and chemical, and second, the energy of the adsorption sites is not the same, ie the adsorbent surface is not uniform [43]:

$$\ln q_e = \ln K_F + \frac{1}{n} \ln C_e \qquad (4)$$

K_F and n are experimental constants where k_F is in terms of ($(mg)^{1-n}$ $L^n g^{-1}$) and is proportional to the adsorption capacity, and n is a unitless quantity and shows the intensity of adsorption

with a range between 0.1 to 1.0. Calculation of K_F and adsorption capacity in Freundlich model shown in (Figure 10).

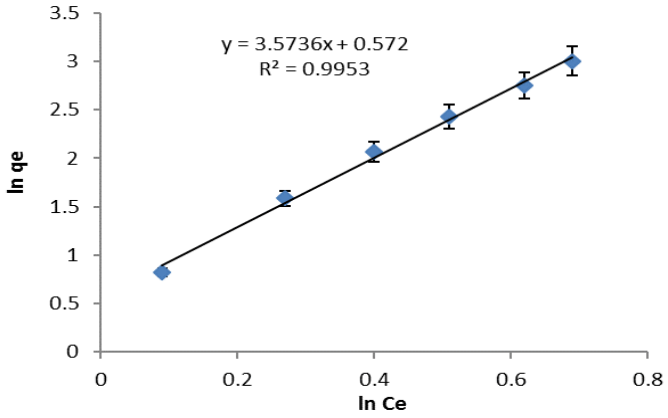

Figure 10. Freundlich isotherm for the adsorption Al (III) ion [Al (III) ion = 50 mg L^{-1}; pH =7.0; dosage sorbent = 0.1 g; time = 90.0 min].

The isotherm model of Temkin (Figure 11), was employed to evaluate indirect adsorbate/adsorbate base on following equation:

$$q_e = \frac{Rt}{b} ln\, K_T + \frac{RT}{b} lnC_e \qquad (5)$$

In this model as mentioned above, R, b, t, K_T and T are the universal gas constant (8.314 J mol^{-1}. K^{-1}), Temkin constant, the heat of the adsorption (J mol^{-1}), the binding constant at equilibrium (L mg^{-1}) and absolute temperature (K) [44].

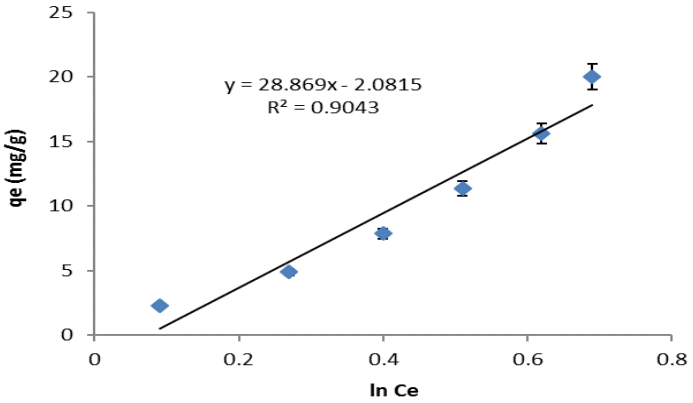

Figure 11. Temkin isotherm for the adsorption Al (III) ion [Al (III) ion = 50 mg L^{-1}; pH =7.0; dosage sorbent = 0.1 g; time = 90.0 min].

Brunoire, Emmett, and Teller isotherm model: Its linear relationship can be used with a good approximation for liquid adsorption based on following equation:

$$\frac{C_e}{(C_s - C_e)q_e} = \frac{1}{K_B q_m} + \frac{K_B - 1}{K_B q_m}\left(\frac{C_e}{C_s}\right) \qquad (6)$$

C_s is the concentration of the adsorbent in the saturated state and can be calculated from the relation $C_s = C_o - C_e$. q_m is the mass of the adsorbent to form a complete layer. K_B is the BET isotherm constant in (g mg^{-1}). Also, K_B is proportional to the energy of the absorbed interaction with the adsorbent (Figure 12, Table 2).

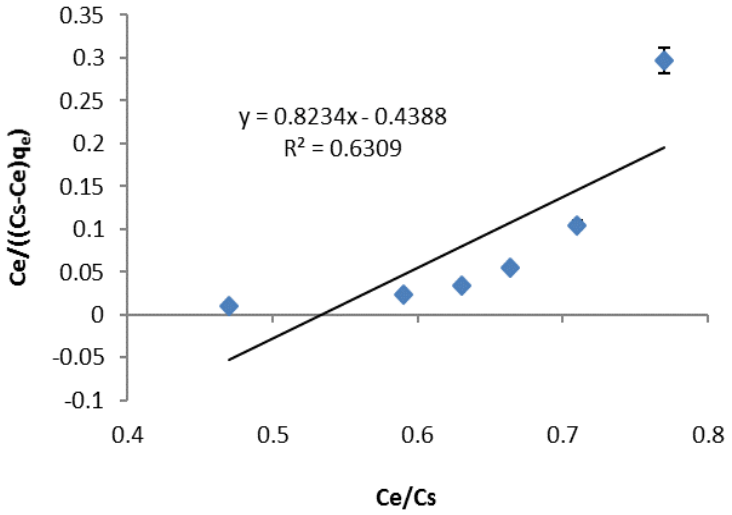

Figure 12. Brunoire, Emmett, and Teller isotherm for the adsorption Al (III) ion [Al (III) ion = 50 mg L^{-1}; pH =7.0; dosage sorbent = 0.1 g; time = 90.0 min].

Table 2. Various isotherm constants for the adsorption Al (III) ion [Al (III) ion = 50 mg L^{-1}; pH =7.0; dosage sorbent = 0.1 g; time = 90.0 min].

Isotherm	parameters	Value of parameters For Al (III) ion
Langmuir	q_m (mgg^{-1})	35.88
	K_L (L mg^{-1})	0.0053
	R^2	0.9503
	X^2	0.94
Freundlich	n	1.008
	K_F $(mg)^{1-n}$ $L^n g^{-1}$	1.762
	R^2	0.9953
	X^2	1.01
Temkin	B_T (J mol^{-1})	12.547
	K_T (L mg^{-1})	1.3
	R^2	0.9043
	X^2	1.12
Brunoire, Emmett, and Teller (BET)	q_m (mgg^{-1})	0.8
	K_B (gmg^{-1})	2.88
	R^2	0.6309
	X^2	1.64

Further discussion about Langmuir isotherm

The removal of Al (III) ion onto CM-β-CD-Fe_3O_4NPs was examined for initial ion concentration range (10 to 100 mg L^{-1}), which is exhibited in (Figure 13). A rise in the initial concentration of Al (III) ion contributes to a rise in the adsorption capacity of these Al (III) ion onto adsorbent. The separation factor (R_L) is the Langmuir constant (L/mg), was calculated using Eq. (9).

$$R_L = \frac{1}{1 + K_L C_0} \qquad (9)$$

The values of R_L can illustrate the shape of the isotherm to be either unfavorable (R_L>1), linear (R_L=1), favorable (0<R_L<1) or irreversible (R_L=0). The plot of the calculated R_L values versus initial concentration of Al (III) ion is shown in (Figure 13) [36,39].

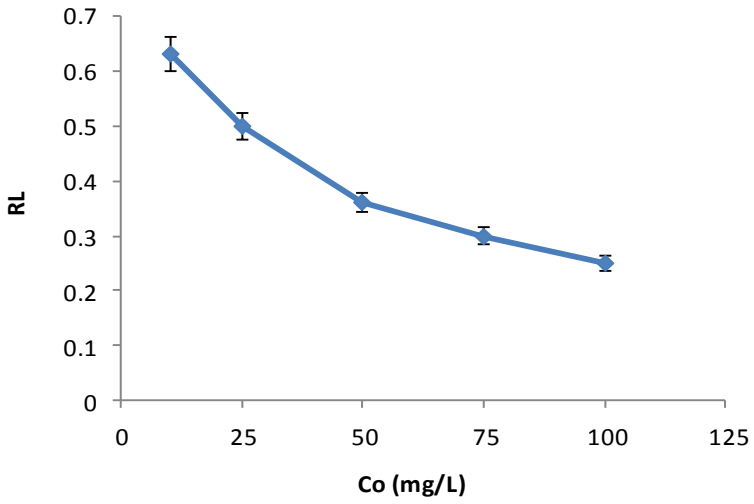

Figure 13. Effect of the Initial Al (III) ion [pH =7.0; dosage sorbent = 0.1 g; time = 90.0 min].

Adsorption kinetic equation

The adsorption kinetic model which is currently commonly used, namely quasi-first-order kinetics and quasi-second-order kinetic adsorption rate model, is used to describe the adsorption rate of adsorbent toward solute. The adsorption mechanism of CM-β-CD-Fe_3O_4NPs toward Al (III) ion can be discussed [46]. The quasi-first-order kinetic model formula is:

$$\ln(q_e - q_t) = \ln q_e - \frac{k_1}{2.303} t \qquad (10)$$

The quasi-second-order dynamic model formula is:

$$\frac{t}{q_t} = \frac{1}{k_2 q_e^2} + \frac{t}{q_e} \qquad (11)$$

Where q_e (mgg^{-1}) is the adsorption equilibrium mass concentration, q_t (mg/g) is the adsorption amount at t time, k_1 is the quasi-first-order rate constant, and k_2 [g/(mg·min)] is the quasi-second-order adsorption rate constant. The obtained kinetic data for adsorption of Al (III) ion onto CM-β-CD-Fe_3O_4NPs an adsorbent were examined with the above mentioned kinetic models shown in (Figure 14, Table 3) [36,46].

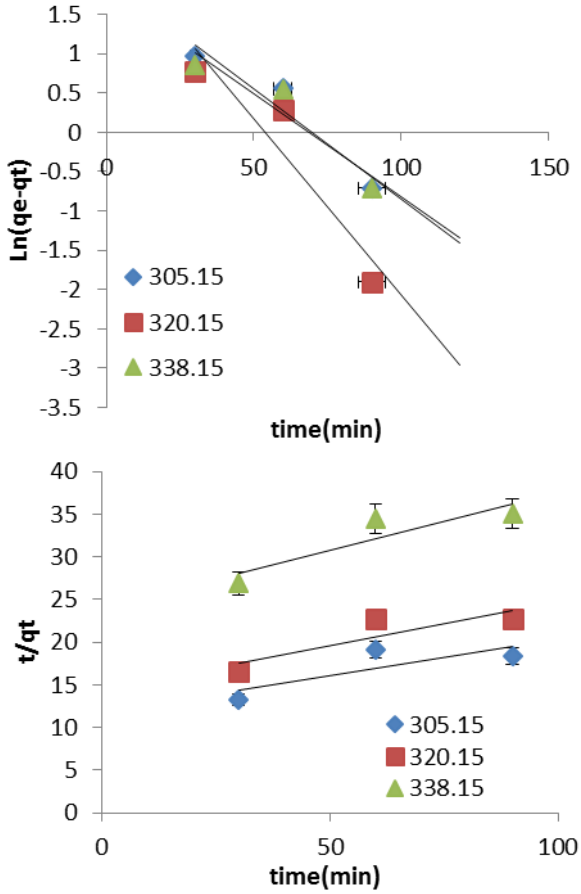

Figure. 14: Juxtaposition of the Kinetic parameters for the adsorption of Al (III) ion [Al (III) ion = 50.0 mg L^{-1}; pH =7.0; dosage sorbent = 0.1 g; time = 90.0 min].

Table 3. Comparison of the Kinetic parameters for the adsorption Al (III) ion [Al (III) ion = 50 mg L^{-1}; pH =7.0; dosage sorbent = 0.1 g; time = 90.0 min].

Model Kinetic	T (^{O}K)	$q_{e\ cal}$ (mgg^{-1})	K_1 (min^{-1})	$q_{e.exp}$ (mgg^{-1})	R^2
pseudo-first-order kinetic	305.15	7.076	0.028	4.985	0.9968
	320.15	10.92	0.0446	4.17	0.9618
	338.15	5.99	0.026	3.56	0.9288

	T (^{O}K)	$q_{e\ cal}$ (mgg^{-1})	k_2 (g (mg^{-1}·min^{-1}))	$q_{e.exp}$ (mgg^{-1})	R^2
pseudo-second-order kinetic	305.15	11.8	6.0×10^{-4}	0.084	0.741
	320.15	12.84	7.04×10^{-4}	0.068	0.8482
	338.15	7.45	7.48×10^{-4}	0.041	0.8987

Thermodynamic study

The standard Gibbs free energy ΔG^0 (kJ mol^{-1}), standard enthalpy change ΔH^0 (kJ mol^{-1}), standard entropy change ΔS^0 (kJ/mol. K) were calculated using the following equations (12) and (13) [46].

$$\Delta G^{\circ} = -RT \ln K_{ad} \qquad (12)$$

$$\ln K_{ad} = \frac{-\Delta H^{\circ}}{RT} + \frac{\Delta S^{\circ}}{R} \qquad (13)$$

Where, T is the temperature in Kelvin, R the gas constant (8.314 J/mol. K), ΔS° and ΔH° values can also be determined from the slope and intercept of the plot of Ln K^0 values 1/T, respectively (Figure 15 and Table 4). The Gibbs free energy (ΔG^0 degree of spontaneity of the adsorption process and the low values reflect an energetically favorable adsorption process. The negative value of (ΔH°) confirms that the sorption process was exothermic in nature and a given amount of heat is evolved during the binding of Al (III) ion onto CM-β-CD-Fe_3O_4NPs the surface of adsorbent. The highly negative ΔS^0 values indicate significant decrease in the degree of randomness at solid/liquid interface during the sorption process [47].

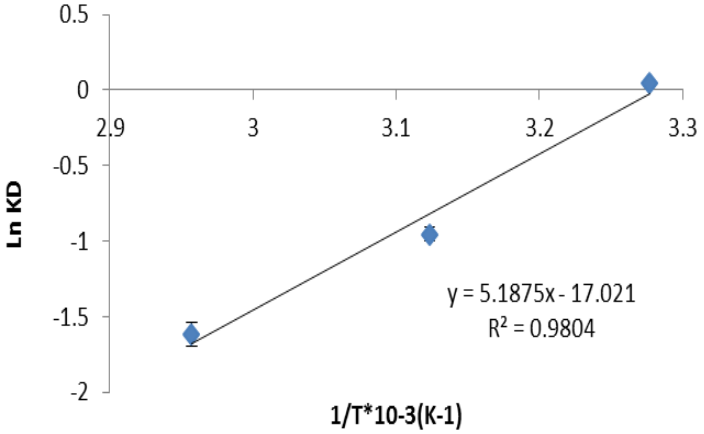

Figure 15. Plot of ln Kc vs. 1/T for the estimation of thermodynamic parameters.

Table 4. The thermodynamic parameters for the adsorption Al (III) ion [Al (III) ion = 50 mg L^{-1}; pH =7.0; dosage sorbent = 0.1 g; time = 90.0 min].

Ion conc. 50 (mg L^{-1})	T (^{O}K)	value of ΔG°(kJ/mol)	value of ΔH°(kJ/mol)	value of ΔS° (kJ/mol K)
Al (III) ion 50 (mg L^{-1})	305.15	-121.006	-42.17	-138.38
	320.15	-2481.46		
	338.15	-4440.44		

Adsorption mechanism of Al (III) ion into CM-β-CD-Fe_3O_4NPs

The physical and chemical characteristics of CM-β-CD-Fe_3O_4NPs were substantially changed by calcination. The specific surface area and the amount of polar functional groups increased, and the adsorption performance improved. Overall, the mechanisms of adsorption of Al (III) ion onto CM-β-CD-Fe_3O_4NPs were mainly attributed to two aspects: chemical adsorption and physical adsorption [22]. Under acid conditions, chemical adsorption is dominant. The carboxyl of Al (III) ion undergoes ion and/or proton exchange reactions with the reactive sites of CM-β-CD-Fe_3O_4NPs with hydroxyl groups. Hydroxyl groups on the adsorbent combine with H^+ in solution, thus resulting in greater hydroxyl group exchange and the formation of ($–OH_2^+$), according to eqn (A). Furthermore, proton exchange reactions occur between $– OH_2^+$ and the hydroxyl group with outer complexes (eqn (B)). Finally, the inner complex is formed by ligand exchange, according to eqn (C) [48].

$$\text{CM-β-CD-Fe}_3\text{O}_4\text{NPs} - \text{OH} + \text{H}^+ \rightarrow \text{CM-β-CD-Fe}_3\text{O}_4\text{NPs} - \text{OH}_2^+ \quad \text{(A)}$$

$$\text{CM-β-CD-Fe}_3\text{O}_4\text{NPs} - \text{OH}_2^+ + \text{Al}^{3+} - \text{C (O) O}^- \leftrightarrow \text{AR} - \text{OH}_2^+\text{O}^- - \text{C (O)} - \text{Al}^{3+} \quad \text{(B)}$$

$$\text{CM-β-CD-Fe}_3\text{O}_4\text{NPs} - \text{OH}_2^+\text{O}^- - \text{C (O)} - \text{Al}^{3+} \leftrightarrow \text{CM-β-CD-Fe}_3\text{O}_4\text{NPs} - \text{OC (O)} - \text{Al}^{3+} + \text{H}_2\text{O} \quad \text{(C)}$$

Recycling of the Adsorbent

The ability of recovering and reusing of the adsorbent was tested in several steps of adsorption and the desorption process were done [49]. The results are shown in (Figure 16). As shown in the figure 98.0% of Al (III) ion was desorbed in the first run and after 6 runs, there were slight changes in Al (III) ion desorption. So, it was concluded that the desired removal of 98% can be achieved after 6 runs.

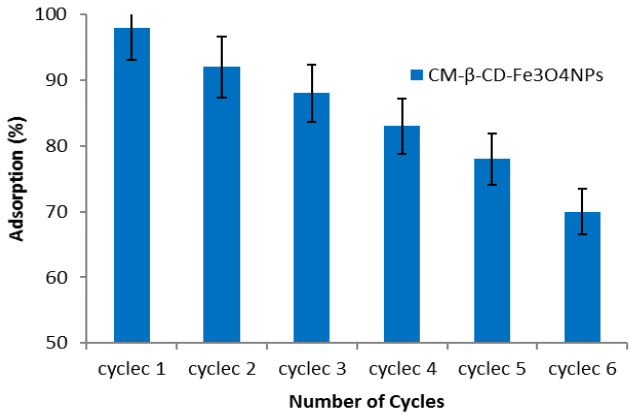

Figure 16. Cycles adsorption of the Al (III) ion [Al (III) ion = 50.0 mg L^{-1}; pH =7.0; dosage sorbent = 0.1 g; time = 90.0 min].

Comparison with other adsorbents for removal Al (III) ion

Table 5 lists a comparison of Al (III) ion adsorption outcomes by the CM-β-CD-Fe_3O_4NPs with those established for its adsorption by other adsorbents in the literature. It can be seen in Table 5 that the CM-β-CD-Fe_3O_4NPs had the highest adsorptive capacity for Al (III) ion in comparison with other adsorbents. This variation in the adsorbed amount of the Al (III) ion could ascribe to various factors, such as the surface area of the adsorbent and pore volume of the adsorbent, types of functional groups that occurred onto its surface, the initial concentration of the Al (III) ion, amount of the adsorbent used, as well as the type of the adsorption mechanism.

Table 5. Comparison for the adsorption of Al (III) ion by batch method.

Ions	Adsorbent	Dosage sorbent	pH	Time	Adsorption capacity	References
Al (III) ion	RHAC	1.0 g	6.0	180 min	34.48 mgg^{-1}	[4]
Al (III) ion	Mn-Fe_2O_4 NPs-AC	0.05 g	5.0	50 min	15.31 mgg^{-1}	[16]
Al (III) ion	R. opacus	0.5 g	5.5	120 min	41.48 mgg^{-1}	[29]
Al (III) ion	Activated carbon (AC)	2.0 g	3.5	120 min	6.56 mgg^{-1}	[40]
Al (III) ion	CM-β-CD-Fe_3O_4NPs	0.1 g	7.0	90 min	35.88 mgg^{-1}	This Work

Conclusion

The application of CM-β-CD-Fe3O4NPs synthesized as adsorbents for the removed of Al (III) ion from waste water. The kinetics and isotherm studies proved the appropriateness of the first-order and Freundlich isotherm models for the kinetics and isotherm of the adsorption of Al (III) ion on the adsorbent. Determination thermodynamic parameters revealed that ΔH˙ values for Al (III) ion is negative, which confirm the exothermic nature of the sorption process. CM-β-CD-Fe_3O_4NPs have a high adsorption capacity when compared to other

adsorbents for Al (III) ion removal from an aqueous medium and an economically viable option that can lead to wastewater treatment advancement and high-quality treated effluent.

Acknowledgement

The authors gratefully acknowledge partial support of this work by the Islamic Azad University, Omidiyeh Branch, Iran.

References

[1] C. Septhum, S. Rattanaphani, J.B. Bremner, V. Rattanaphani, *J. Hazar. Mater.,* 148, 185 (2007).

[2] C.G. Kim, *Asian. J. Chem.,* 25, 5884 (2013).

[3] P. Karthikeyan, S. Vigneshwaran, S. Meenakshi, *Environ. Chem. Ecotoxicol.,* 2, 97 (2020).

[4] N.T. Abdel-Ghani, G.A. El-Chaghaby, E.M. Zahran, *American J. Anal. Chem.,* 6, 71 (2015).

[5] A.A. Huseyinli, R. Alieva, S. Haciyeva, T. Guray, *J. Hazar. Mater.,* 163, 1001 (2009).

[6] J. Malik, A. Frankova, O. Drabek, J. Szakova, C. Ash, L. Kokoska, *J. Food. Chem.,* 139, 728 (2013).

[7] V.N. Bulut, D. Arslan, D. Ozdes, M. Soylak, M. Tufekci, *J. Hazar. Mater.,* 182, 331 (2010).

[8] A. Shokrollahi, M. Ghaedi, M.S. Niband, H.R. Rajabi, *J. Hazar. Mater.,* 151, 642 (2008).

[9] H. Ciftci, C. Er, *Environ. Monit. Ass.,* 185, 2745 (2013).

[10] S.H. Abbasi, A. Farmany, M.B. Gholivand, A. Naghipour, F. Abbasi, H. Khani, *J. Food. Chem.,* 116, 1019 (2009).

[11] S. Tontrong, S. Khonyoung, S. Jakmunee, *J. Food. Chem.,* 132, 624 (2012).

[12] R. Hakimelahi, K. Niknam, *Eur. J. Anal. Chem.,* 12, 963 (2017).

[13] R. Jalili, A. Khataee, *Microchimica Acta.,* 186, 29 (2019).

[14] M.C. Shinzato, R. Hypolito, *Environ. Earth. Sci.,* 75, 1 (2016).

[15] P. Nasehi, M.S. Moghaddam, S.F. Abbaspour, N. Karachi, *Separa. Sci. Technol.,* 55, 1078 (2019).

[16] M.A. Badawi, N.A. Negm, M.T.H. Abou Kana, H.H. Hefni, M.M. Abdel Moneem, *Int. J. Biolog. Macromol.,* 99, 465 (2017).

[17] B.B.A. Francisco, L.F.S. Caldas, D.M. Brum, R.J. Cassella, *J. Hazar. Mater.,* 181, 485 (2010).

[18] I.O. Igbokwe, E. Igwenagu, N.A. Igbokwe, *Interdiscip. Toxicol.*, 12, 45 (2019).

[19] D. Popugaeva, K. Manoli, K. Kreyman, A.K. Ray, *J. Mech. Composite Mater.*, 25, 1575 (2019).

[20] K. B. L. Borchert, R. Boughanmi, B. Reis, P. Zimmermann, Ch. Steinbach, P. Graichen, A. Svirepa, J. Schwarz, R. Boldt, S. Schwarz, M. Mertig, D. Schwarz, *Polysacchar.*, 2, 429 (2021).

[21] N. Nourbakhsh, H. Zavvar mousavi, E. Kolivari, A. Khaligh, *Chem. Ind. Chem. Eng.*, 25, 107 (2019).

[22] M. Rahmani Piani, M. Abrishamkar, B. Mombeni Goodajdar, M. Hossieni, *Desal. Water Treat.*, 213, 228 (2021).

[23] P. Nasehi, B. Mahmoudi, S.F. Abbaspour, M.S. Moghaddam, *RSC. Adv.*, 9, 20087 (2020).

[24] H.S. Ghazimokri, M. Monajjemi, H. Aghaie, *Rev. De La Univer. Del Zul.*, 29, 98 (2020).

[25] K. Liu, H. Liu, L. Li, W. Li, J. Liu, T. Tang, *Supramol. Chem.*, 33(4), 1 (2021). http://doi.org.1080/10610278.2021.1917574.

[26] A.Z.M. Badruddoza, Z. B. Z. Shawon, W. J. D. Tay, K. Hidajat, M. S. Uddin, *Polymers.*, 91, 322 (2013).

[27] H. S. Ghazimokri, H. Aghaie, M. Monajjemi, M. R. Gholami, *Russian J. Phys. Chem. A.*, 96, 371 (2022).

[28] B. Mombeni Goodajdar, F. Marahel, L. Niknam, E. Pournamdari, E. Mousavi, *Int. J. Environ. Anal. Chem.*, 101, 1 (2021). https://doi.org/10.1080/03067319.2021.1940159.

[29] J.E.B. Cayllahua, M.L. Torem, *J. Chem. Eng.*, 161, 1 (2010).

[30] S. Cao, Y. Cao, Z. Ma, Y. Liao, *Physicochem. Prob. Miner. Proc.*, 55, 97 (2019).

[31] M. Jemeljanova, R. Ozola, M. Klavins, *Agron. Res.*, 17, 1023 (2019).

[32] G. Mamba, X.Y. Mbianda, P.P. Govender, B.B. Mamba, R.W. Krause, *J. Appl. Sci.*, 10, 940 (2010).

[33] A. Mittal, R. Ahmad, I. Hasan, *Desal. Water. Treat.*, 57, 15133 (2016).

[34] S. Bagheri, H. Aghaei, M. Ghaedi, A. Asfaram, M. Monajemi, A.A. Bazrafshan, *Ultrasonics- Sonochem.*, 41, 279 (2018).

[35] A. A. Oladipo, M. Gazi, *Chem. Eng. Res. Des.*, 121, 329 (2017).

[36] A. A. Ghazali, F. Marahel, B. Mombeni Goodajdar, *Int. J. Environ. Anal. Chem.*, 101, 1 (2021). https://doi.org/10.1080/03067319.2021.1953492.

[37] P. Karunasri Meghana, A. A. Kumari, K. Venkata Pravalika, P. Janaki Sriram, K. Ravindhranath, *Ras. J. Chem.*, 12, 338 (2019).

[38] B. Kaboudin, M. Torabi Momen, F. Kazemi, P. Ray, *Anal. Chem.,* 7, 1 (2021). doi: 10.26434/chemrxiv.14707251.v1.

[39] Z. Kazemi, F. Marahel, T. Hamoule, B. Mombeni Goodajdar, *Desal. Water Treat.,* 213, 381 (2021).

[40] S. Lunge, S. Singh, A. Sinha, *J. Magn. Magn. Mater.*, 356, 21 (2014).

[41] V. Jonasi, K. Matina, U. Guyo, *Turk. J. Chem.*, 41, 748 (2017).

[42] T. Mahmood, M. Aslam, A. Naeem, T. Siddique, S. Ud. Din, *J. Chil. Chem. Soc.*, 63, 3855 (2018).

[43] Z. Aly, A. Graulet, N. Scales, T. Hanley, *Environ. Sci. Pollut. Res.*, 21, 3972 (2014).

[44] F. Ntuli, T. Falayi, C. Mabasa, *Environ. Agric. Sci.*, 270, 229 (2014).

[45] S. Brunauer, P.H. Emmett, E. Teller, *J. Am. Chem. Soc.,* 60, 309 (1938).

[46] B. Thalmann, U. Von Gunten, R. Kaegi, *J. Water Res.*, 134, 170 (2018).

[47] R. Padash, E. Jamalizadeh, A.H. Jafari, *Mater.,* 64, 550 (2017).

[48] A.H. Jawad, A.S. Abdulhameed, S.N. Surip, S. Sabar, *Int. J. Environ. Anal. Chem.,* 100, 1 (2020). https://doi.org/10.1080/03067319.2020.1807966.

[49] S.M. Mousavi, S.A. Hashemi, H. Esmaeili, A.M. Amani, F. Mojoudi, *Acta Chim. Slov.,* 65, 750 (2018).